CARDIFF UNIVERSITY PRIFYSGOL CAERDYDD

ORCA – Online Research @ Cardiff

This is an Open Access document downloaded from ORCA, Cardiff University's institutional repository:https://orca.cardiff.ac.uk/id/eprint/145826/

This is the author's version of a work that was submitted to / accepted for publication.

Citation for final published version:

Jang, Hyeon-Sik, Kim, Tae-Hoon, Kim, Byeong Geun, Hou, Bo , Lee, In-Hwan, Jung, Su-Ho, Lee, Jae-Hyun, Cha, SeungNam, Yang, Cheol-Woong, Kim, Byung-Sung and Whang, Dongmok 2021. Self-catalytic growth of elementary semiconductor nanowires with controlled morphology and crystallographic orientation. Nano Letters 21 (23) , pp. 9909-9915. 10.1021/acs.nanolett.1c02982

Publishers page: http://dx.doi.org/10.1021/acs.nanolett.1c02982

Please note:
Changes made as a result of publishing processes such as copy-editing, formatting and page numbers may not be reflected in this version. For the definitive version of this publication, please refer to the published source. You are advised to consult the publisher's version if you wish to cite this paper.

This version is being made available in accordance with publisher policies. See http://orca.cf.ac.uk/policies.html for usage policies. Copyright and moral rights for publications made available in ORCA are retained by the copyright holders.

Self-catalytic growth of Elementary Semiconductor Nanowires with Controlled Morphology and Crystallographic Orientation

Hyeon-Sik Jang[1], Tae-Hoon Kim[1,2], Byeong Geun Kim[3], Bo Hou[4], In-Hwan Lee[1], Su-Ho Jung[1], Jae-Hyun Lee[5], SeungNam Cha[6], Cheol-Woong Yang[1], Byung-Sung Kim[1,7] and Dongmok Whang[1]**

[1]School of Advanced Materials Science and Engineering and SKKU Advanced Institute of Nanotechnology, Sungkyunkwan University, Suwon 16419, Korea

[2]Department of Materials Science and Engineering, Chonnam National University, Gwangju 61186, Republic of Korea

[3]Research Development Division Materials and Components Research Team, Gyeongbuk Institute of IT Convergence Industry Technology, Kyungsan 38463, Korea

[4]Department of Physics and Astronomy, Cardiff University, Cardiff CF24 3AA, United Kingdom

[5]Department of Energy Systems Research and Department of Materials Science and Engineering, Ajou University, Suwon 16499, Korea

[6]Department of Physics, Sungkyunkwan University, Suwon 16419, Korea

[7]Department of Engineering Science, University of Oxford, Parks Road, Oxford OX1 3PJ, UK

Abstract: While the orientation-dependent properties of semiconductor nanowires have been theoretically predicted, their study has long been overlooked in many fields owing to the limits to control the crystallographic growth direction of nanowires (NWs). We present here the orientation-controlled growth of single-crystalline germanium (Ge) NWs using a self-catalytic low-pressure chemical vapor deposition process. By adjusting the growth temperature, the orientation of growth direction in GeNWs was selectively controlled to the <110>, <112>, or <111> directions on the same substrate. The NWs with different growth directions exhibit distinct morphological features, allowing control of the NW morphology from uniform NWs to nanoribbon structures. Significantly, the VLS-based self-catalytic growth of the <111> oriented GeNW suggests that NW growth is possible for single elementary materials even without an appropriate external catalyst. Furthermore, these findings could provide opportunities to investigate the orientation-dependent properties of semiconductor NWs.

Keywords: chemical vapor deposition, germanium, nanowire, orientation control, self-catalytic growth.

Semiconductor NWs are promising building blocks for nanoscale electronic and optoelectronic applications due to their unique one-dimensional structure, quantum confinement effects, and compatibility with existing semiconductor technologies.[1-4] Over the past two decades, varieties of semiconductor NWs have been realized through well-developed growth techniques which allow control of the structures, morphologies, and compositions.[5-10] However, the crystallographic control over the growth orientations of semiconductor NWs remains a significant challenge. Numerous theoretical and experimental studies have suggested that the properties of NW are strongly dependent on its crystallographic direction. For example, theoretically, the specific crystal orientations might induce a unique electronic structure with an indirect-to-direct energy gap transition and enhanced carrier mobility under strong quantum confinement effects.[11-14] Experimental studies have also revealed that the crystal orientations of semiconductor NWs have a significant role in determining the different mechanical, piezoelectric, and photovoltaic properties of NW-based electronic and energy-harvesting devices.[15-18] These studies related to orientation-dependent properties of NWs have provoked investigations for control of NW orientation via metal catalyst engineering, templated synthesis, or metal-assisted chemical etching.[19-24] In particular, the preferred growth direction of the NWs grown by vapor-liquid-solid (VLS) growth and oxide-assisted growth (OAG) have been intensively studied. In group-IV elementary semiconductors, such as Si and Ge, single-crystalline NWs grown by VLS approach using metal catalyst predominantly grow along the <111> direction.[25-26] In contrast, <112> or <110> directions are energetically favored for NWs grown using the OAG process.[27-28] In our previous study, a self-catalytic growth method was suggested to synthesize single-crystalline silicon (Si) and germanium (Ge) NWs.[29] Control over the diameter and in-situ doping of the semiconductor NWs also demonstrated that this method is well suited for electronic device

applications. Here, we demonstrate that the orientation of the self-catalytic GeNWs can be controlled with the <110>, <112>, and <111> growth directions. Through a detailed analysis of the NW growth phenomena, the growth mechanism and the crystal orientation dependence of the GeNWs were investigated. In particular, in-depth studies for the growth behavior and the morphology of <111> oriented NWs strongly suggest the NWs have been grown through the self-catalytic VLS process. Furthermore, the NWs with different growth directions exhibit distinct morphological features, allowing control of the NW morphology from uniform NWs to 2D-like NRs structures.

Self-catalytic GeNWs grown at low temperature (T_g < 320 °C) with the high partial pressure of Ge precursor (GeH_4) have random growth directions (Fig. S1 in supporting information). However, under low GeH_4 partial pressure, NWs predominantly grow in a specific crystallographic direction, and the direction can be controlled according to the growth temperature even on the same substrate (Fig. 1). The scanning electron microscope (SEM) image in Figure 1a shows uniform GeNWs grown at 340 °C. When viewed along the [100] direction of the substrate plane, the GeNWs are inclined at 45 °C and are consistent with the <110> growth direction. At 360 °C, most NWs are grown along the <112> direction with a slightly tapered morphology (Fig. 1b). The GeNWs grown at temperatures above 380 °C are aligned at a 90° angle normal to the substrate with the four fixed <111> directions, indicating the NWs are <111> oriented (Fig. 1c). Figures 1d-f show high-resolution transmission electron microscope (HRTEM) images and selected area electron diffraction (SAED) patterns near the tips of the <110>, <112>, and <111> oriented single-crystalline GeNWs, respectively. The temperature dependence of the NW growth direction was further verified by the change in the NW growth direction according to the temperature change during growth (Fig. 2b and Fig. S2). Initially, <112>-oriented GeNWs having

a rectangular cross-section were grown at 360 °C. When increasing the temperature up to 420 °C during the growth, the growth direction changes from <112> to <111>, and the cross-sectional shape was also changed from rectangular to hexagonal shape.

Based on the results, a possible mechanism for the orientation-controlled NW growth is suggested (Fig. 2a). When supersaturation in the gas phase reaches a critical level, Ge nanocrystal seeds can be nucleated on the reactive oxide surface.[29] At low growth temperature, the subsequent formation of stable side facets promotes the anisotropic growth in the <110> or <112> direction as precursor species are continuously supplied to the Ge nanowire tip with a high sticking coefficient. In general, spontaneous growth of crystalline NWs usually progresses in a direction that shows minimal surface energy at the NW growth tip. Among the low-index facets of Si and Ge with diamond cubic structure, the {111} and {100} facets have the lowest and second-lowest surface energy, respectively,[30] and thus <112> or <110> growth directions with {111} and {100} side facets are energetically favored for the group IV semiconductor NWs grown without an external catalyst.[27-28, 31] The related thermodynamic studies have been systematically conducted in the Si and Ge NWs.[32-33] As the temperature increases to 380 °C, the NW tips are presumed to exist as a fully liquid state due to size-dependent melting point depression. Bulk Ge crystal has a high melting temperature (937 °C). However, an in-situ TEM study recently demonstrated that Ge nanoparticles with a diameter of approximately 20 nm readily melt even at temperatures below 400 °C.[34-35] Because the liquid-solid interface at the growth tip prefers {111} solid facets with the lowest interface energy,[36] GeNWs can grow in the <111> growth directions perpendicular to the {111} surfaces, although the surface energy of NW sidewall is higher than that of NWs grown in <110> and <112> directions (Fig. S3). For Si and Ge NWs, the <111> growth direction is a unique feature observed only in VLS and VLS-like growth to the best of our knowledge.[5, 32, 37]

Furthermore, the <111>-oriented GeNWs with connected chain-like morphology were occasionally observed at the high growth temperature (Fig. S4). The lamellar twinning periodically occurs in the narrow neck of the spherical chains,[38-41] which is due to 2D ledge nucleation and epitaxial propagation occurring along the liquid-solid {111} interface.[42-43] Similar phenomena are also observed in crystal growth of undercooled Ge melt, favoring closed-packed {111} facets at the liquid-solid interface.[44-45] In general, compound solids, such as II-VI or III-V semiconductors, can grow anisotropically to 1D NWs through the VLS process even without an external catalyst because one of the elements can act as a liquid catalyst during the NW growth. However, VLS-based 1D growth of single-element materials has been limitedly studied only in materials, such as Si and Ge, for which suitable external metal catalysts are available.

To investigate the orientation-dependent structural features, GeNWs with <110>, <112>, and <111> crystal directions were synthesized under GeH_4 partial pressure of 1.5 Torr with the flow rate of 40 sccm at 380°C (Fig. 3a). Although grown under the same conditions, the NWs exhibited characteristic morphological features depending on the crystal growth direction (Fig. 3b). While the <111>-oriented GeNWs are highly tapered with a relatively low growth rate, the <110>-oriented GeNWs had a much faster growth rate and uniform diameter. The <112>-oriented GeNW showed a moderate growth rate and tapering. Furthermore, it is worth mentioning that the axial and radial growth rates of GeNWs were strongly dependent on their crystallographic growth directions, which have rarely been studied before. These interesting phenomena can be explained by the geometric and thermodynamic properties of the semiconductor NWs enclosed by the crystal facets with different surface energies. The {112} side plane enclosing <111>-oriented GeNW with hexagonal cross-section has relatively higher surface energy compared with the other low-index planes.[46] Therefore, Ge adatoms from the vapor precursor species are easily incorporated at the

side planes, promoting the radial growth in the <111> oriented GeNWs (Fig. 3c). On the other hand, <110> oriented GeNWs have the lowest-energy state owing to the presence of three {111} and three {100} stable planes.[31] Direct precursor impingement for radial growth is suppressed, and Ge adatoms easily diffuse up to the NW tip. As a result, the growth rate in the axial direction is much faster even under the same growth conditions, resulting in a uniform shape of <110> oriented GeNWs (Fig. 3e). The <112> oriented GeNW has a rectangular cross-section which consists of two {111} and two {110} side planes.[47] The slightly tapered morphology is related to the thermodynamic lateral growth on a specific side surface (Fig. 3d).

The highly tapered GeNWs growing along the [111] direction have sawtooth faceting along the entire NW length (Fig.4a and Fig. S5). The periodicity of upward and downward {111} facets is observed, accompanying high-index planes such as $(11\bar{5})$, $(55\bar{7})$, and $(11\bar{9})$ on the side surface of each {112} of the [111] oriented GeNW (Figs. 4c-e). This periodic faceting has often been observed in semiconductor NWs grown *via* metal-catalyzed VLS growth, and it has been attributed to liquid-solid instability, enhanced vapor-solid (VS) deposition, impurity diffusion, or other chemical species supplied from the gas phase.[46, 48-50] However, the downward faceting observed at the base of <111> oriented GeNWs indicates that the periodic faceting results from the competition between interfacial instability and surface energy minimization at the high temperature (Fig. S6). The surface energy of {112} side planes increases with the elongation of the NWs, leading to the periodic formation of the (111)/(002) plane to stabilize the radial growth perpendicular to the liquid-solid interface of the <111> oriented GeNWs. In addition, continuous VS deposition at a high temperature can induce surface reconstruction on a side plane, resulting in the formation of the high-index planes.[51-52] In contrast to the highly tapered <111> oriented GeNW, <110> oriented GeNW has very uniform morphology along the axial direction because

the <110> oriented NWs are bounded by a large number of {111} and {110} planes having the lowest surface energy (Figs. 4f-h).[53-54] Therefore, unintentional Ge deposition on <110> oriented GeNWs could be minimized, thus preventing the formation of tapered morphology of non-uniform dopant distribution along the NW length.[55-56] Theoretical and experimental studies have also reported that stable <110> NWs can have significantly increased carrier mobility,[57-58] indicating that the selective preparation of <110> oriented NWs may improve reliability as well as performance in electronic device applications of semiconducting NWs. Otherwise, the <112>-oriented NW of group-IV materials usually has a rectangular cross-section, and its sides consist of two low-energy {111} and high-energy {110} surfaces.[47] By taking advantage of the energy difference between the two different facets, we have grown flexible 2D-like GeNRs (Figs. 4i-k). Ge species can be preferentially adsorbed on unstable {110} planes, eventually leading to morphological evolution from <112> oriented GeNWs to GeNRs. The large width to thickness ratio also reveals that the lateral growth on the {110} planes simultaneously occurs and competes with the axial growth of the <112> NWs (Fig. S7). To further investigate the anisotropic lateral growth of the <112> oriented GeNWs, we enhanced lateral growth of the <112> NWs to <110> directions using a two-step process, which clearly shows that different surface energies promote the preferential growth on the {110} planes (Fig. S8). 2D semiconductor NRs are promising building blocks for flexible or stretchable electronics.[59-60] However, bottom-up grown NRs have seldom been observed in group-IV semiconductor materials.

In conclusion, we demonstrated that the crystal orientation of self-catalytic GeNWs could be selectively controlled by adjusting the growth temperature. At low temperature, the <110> oriented GeNWs mainly grow with a uniform diameter along the NW length, while at high-temperature growth, the <111> oriented GeNWs exhibit a highly tapered morphology. At an intermediate

temperature, the <112> oriented GeNWs predominantly grow. We also demonstrated that different crystal orientations play an essential role in determining the geometrical and morphological features of NWs. In particular, the controlled evolution from rectangular GeNWs to flexible 2D-like GeNRs is an excellent example of the morphology-controlled growth of novel nanostructures. The results of this study may provide an opportunity to utilize the orientation-dependent properties of semiconductor NW in practical device applications. Furthermore, the self-catalytic growth of the <111> oriented Ge NWs suggests VLS-based NW growth may be possible for a wide range of single elementary materials even without an external catalyst.

Supporting Information

Detailed experimental procedures and Figures S1− S8. The Supporting Information is available free of charge at http://pubs.acs.org.

Corresponding Author

*E-Mail: dwhang@skku.edu (D.W); skku97@gmail.com (B.-S.K.)

Notes

The authors declare no competing financial interest.

Acknowledgment

This research was supported by the National Research Foundation (NRF-2021R1A2C2013378) of the Ministry of Science and ICT of Korea and the Korea Basic Science Institute (KBSI) National Research Facilities & Equipment Center (NFEC) grant funded by the Korea Ministry of Education (No. 2019R1A6C1010031). BK acknowledges support from Basic Science Research Program

through the National Research Foundation of Korea (NRF) funded by the Ministry of Education (2013R1A6A3A03063814).

References

1. Cui, Y.; Lieber, C. M., Functional nanoscale electronic devices assembled using silicon nanowire building blocks. *Science* **2001,** *291*, 851-853.
2. Jin, S.; Whang, D.; McAlpine, M. C.; Friedman, R. S.; Wu, Y.; Lieber, C. M., Scalable interconnection and integration of nanowire devices without registration. *Nano Lett.* **2004,** *4*, 915-919.
3. Yan, R.; Gargas, D.; Yang, P., Nanowire photonics. *Nat. Photonics* **2009,** *3*, 569-576.
4. Cui, Y.; Wei, Q.; Park, H.; Lieber, C. M., Nanowire nanosensors for highly sensitive and selective detection of biological and chemical species. *Science* **2001,** *293*, 1289-1292.
5. O'Regan, C.; Biswas, S.; Petkov, N.; Holmes, J. D., Recent advances in the growth of germanium nanowires: Synthesis, growth dynamics and morphology control. *J. Mater. Chem. C* **2014,** *2*, 14-33.
6. Lauhon, L. J.; Gudlksen, M. S.; Wang, D.; Lieber, C. M., Epitaxial core-shell and core-multishell nanowire heterostructures. *Nature* **2002,** *420*, 57-61.
7. Yang, J. E.; Jin, C. B.; Kim, C. J.; Jo, M. H., Band-gap modulation in single-crystalline $Si_{1-x}Ge_x$ nanowires. *Nano Lett.* **2006,** *6*, 2679-2684.
8. Gudiksen, M. S.; Lauhon, L. J.; Wang, J.; Smith, D. C.; Lieber, C. M., Growth of nanowire superlattice structures for nanoscale photonics and electronics. *Nature* **2002,** *415*, 617-620.
9. Nguyen, B. M.; Taur, Y.; Picraux, S. T.; Dayeh, S. A., Diameter-independent hole mobility in Ge/Si Core/shell nanowire field effect transistors. *Nano Lett.* **2014,** *14*, 585-591.
10. Park Ii, W.; Zheng, G.; Jiang, X.; Tian, B.; Lieber, C. M., Controlled synthesis of millimeter-long silicon nanowires with uniform electronic properties. *Nano Lett.* **2008,** *8*, 3004-3009.
11. Filonov, A. B.; Petrov, G. V.; Novikov, V. A.; Borisenko, V. E., Orientation effect in electronic properties of silicon wires. *Appl. Phys. Lett.* **1995,** *67*, 1090.
12. Persson, M. P.; Lherbier, A.; Niquet, Y. M.; Triozon, F.; Roche, S., Orientational dependence of charge transport in disordered silicon nanowires. *Nano Lett.* **2008,** *8*, 4146-4150.
13. Arantes, J. T.; Fazzio, A., Theoretical investigations of Ge nanowires grown along the [110] and [111] directions. *Nanotechnology* **2007,** *18*, 295706.
14. Yang, X. B.; Zhang, R. Q., Indirect-to-direct band gap transitions in phosphorus adsorbed <112> silicon nanowires. *Appl. Phys. Lett.* **2008,** *93*, 173108

15. Dellas, N. S.; Liu, B. Z.; Eichfeld, S. M.; Eichfeld, C. M.; Mayer, T. S.; Mohney, S. E., Orientation dependence of nickel silicide formation in contacts to silicon nanowires. *J. Appl. Phys.* **2009,** *105*, 094309.
16. Yang, H.; Huang, S.; Huang, X.; Fan, F.; Liang, W.; Liu, X. H.; Chen, L. Q.; Huang, J. Y.; Li, J.; Zhu, T.; Zhang, S., Orientation-dependent interfacial mobility governs the anisotropic swelling in lithiated silicon nanowires. *Nano Lett.* **2012,** *12*, 1953-1958.
17. Zhao, Q.; Xie, T.; Peng, L.; Lin, Y.; Wang, P.; Peng, L.; Wang, D., Size- and orientation-dependent photovoltaic properties of ZnO nanorods. *J. Phys. Chem. C* **2007,** *111*, 17136-17145.
18. Li, X.; Wei, X.; Xu, T.; Pan, D.; Zhao, J.; Chen, Q., Remarkable and crystal-structure-dependent piezoelectric and piezoresistive effects of InAs nanowires. *Adv. Mater.* **2015,** *27*, 2852-2858.
19. Adhikari, H.; Marshall, A. F.; Chidsey, C. E. D.; McIntyre, P. C., Germanium nanowire epitaxy: Shape and orientation control. *Nano Lett.* **2006,** *6*, 318-323.
20. Lugstein, A.; Steinmair, M.; Hyun, Y. J.; Hauer, G.; Pongratz, P.; Bertagnolli, E., Pressure-induced orientation control of the growth of epitaxial silicon nanowires. *Nano Lett.* **2008,** *8*, 2310-2314.
21. Shimizu, T.; Xie, T.; Nishikawa, J.; Shingubara, S.; Senz, S.; Gösele, U., Synthesis of vertical high-density epitaxial Si(100) nanowire arrays on a Si(100) substrate using an anodic aluminum oxide template. *Adv. Mater.* **2007,** *19*, 917-920.
22. Wang, J.; Plissard, S. R.; Verheijen, M. A.; Feiner, L. F.; Cavalli, A.; Bakkers, E. P. A. M., Reversible switching of InP nanowire growth direction by catalyst engineering. *Nano Lett.* **2013,** *13*, 3802-3806.
23. Zhang, M. L.; Peng, K. Q.; Fan, X.; Jie, J. S.; Zhang, R. Q.; Lee, S. T.; Wong, N. B., Preparation of large-area uniform silicon nanowires arrays through metal-assisted chemical etching. *J. Phys. Chem. C* **2008,** *112*, 4444-4450.
24. Tsivion, D.; Schvartzman, M.; Popovitz-Biro, R.; Von Huth, P.; Joselevich, E., Guided growth of millimeter-long horizontal nanowires with controlled orientations. *Science* **2011,** *333*, 1003-1007.

25. Huang, Y. H., Competition between surface energy and interphase energy in transition region and diameter-dependent orientation of silicon nanowires. *Appl. Surf. Sci.* **2009,** *255*, 4347-4350.
26. Schmidt, V.; Senz, S.; Gösele, U., Diameter-dependent growth direction of epitaxial silicon nanowires. *Nano Lett.* **2005,** *5*, 931-935.
27. Tan, T. Y.; Lee, S. T.; Gösele, U., A model for growth directional features in silicon nanowires. *Appl. Phys. A* **2002,** *74*, 423-432.
28. Zhang, R. Q.; Lifshitz, Y.; Lee, S. T., Oxide-assisted growth of semiconducting nanowires. *Adv. Mater.* **2003,** *15*, 635-640.
29. Kim, B. S.; Koo, T. W.; Lee, J. H.; Kim, D. S.; Jung, Y. C.; Hwang, S. W.; Choi, B. L.; Lee, E. K.; Kim, J. M.; Whang, D., Catalyst-free growth of single-crystal silicon and germanium nanowires. *Nano Lett.* **2009,** *9*, 864-869.
30. Stekolnikov, A. A.; Furthmüller, J.; Bechstedt, F., Absolute surface energies of group-IV semiconductors: Dependence on orientation and reconstruction. *Phys. Rev. B* **2002,** *65*, 115318.
31. Hanrath, T.; Korgel, B. A., Crystallography and surface faceting of germanium nanowires. *Small* **2005,** *1*, 717-721.
32. Garcia-Gil, A.; Biswas, S.; Holmes, J. D., A Review of Self-Seeded Germanium Nanowires: Synthesis, Growth Mechanisms and Potential Applications. *Nanomaterials* **2021,** *11*, 2002.
33. Migas, D. B.; Borisenko, V. E.; Rusli; Soci, C., Revising morphology of <111>-oriented silicon and germanium nanowires. *Nano Converg.* **2015,** *2*, 16.
34. Hassion, F. X.; Thurmond, C. D.; Trumbore, F. A., On the melting point of germanium. *J. Phys. Chem. C* **1955,** *59*, 1076-1078.
35. Lotty, O.; Hobbs, R.; O'Regan, C.; Hlina, J.; Marschner, C.; O'Dwyer, C.; Petkov, N.; Holmes, J. D., Self-seeded growth of germanium nanowires: Coalescence and ostwald ripening. *Chem. Mater.* **2013,** *25*, 215-222.
36. Wang, H.; Zepeda-Ruiz, L. A.; Gilmer, G. H.; Upmanyu, M., Atomistics of vapour–liquid–solid nanowire growth. *Nat. Commun.* **2013,** *4*, 1956.
37. Schmidt, V.; Wittemann, J. V.; Senz, S.; Gösele, U., Silicon Nanowires: A Review on Aspects of their Growth and their Electrical Properties. *Adv.Mater.* **2009,** *21*, 2681-2702.

38. Fujiwara, K., Crystal growth behaviors of silicon during melt growth processes. *Int. J. Photoenergy* **2012,** *2012*, 169829.

39. Hao, Y.; Meng, G.; Wang, Z. L.; Ye, C.; Zhang, L., Periodically twinned nanowires and polytypic nanobelts of ZnS: The role of mass diffusion in vapor-liquid-solid growth. *Nano Lett.* **2006,** *6*, 1650-1655.

40. Kutsukake, K.; Abe, T.; Usami, N.; Fujiwara, K.; Morishita, K.; Nakajima, K., Formation mechanism of twin boundaries during crystal growth of silicon. *Scr. Mater.* **2011,** *65*, 556-559.

41. Xiong, Q.; Wang, J.; Eklund, P. C., Coherent twinning phenomena: Towards twinning superlattices in III-V semiconducting nanowires. *Nano Lett.* **2006,** *6*, 2736-2742.

42. Hofmann, S.; Sharma, R.; Wirth, C. T.; Cervantes-Sodi, F.; Ducati, C.; Kasama, T.; Dunin-Borkowski, R. E.; Drucker, J.; Bennett, P.; Robertson, J., Ledge-flow-controlled catalyst interface dynamics during Si nanowire growth. *Nat. Mater.* **2008,** *7*, 372-375.

43. Wen, C. Y.; Reuter, M. C.; Tersoff, J.; Stach, E. A.; Ross, F. M., Structure, growth kinetics, and ledge flow during vapor-solid-solid growth of copper-catalyzed silicon nanowires. *Nano Lett.* **2010,** *10*, 514-519.

44. Nagashio, K.; Kuribayashi, K., Growth mechanism of twin-related and twin-free facet Si dendrites. *Acta Mater.* **2005,** *53*, 3021-3029.

45. Herlach, D. M.; Simons, D.; Pichon, P.-Y., Crystal growth kinetics in undercooled melts of pure Ge, Si and Ge-Si alloys. *Philos. Trans. Royal Soc. A* **2018,** *376*, 20170205.

46. Ross, F. M.; Tersoff, J.; Reuter, M. C., Sawtooth faceting in silicon nanowires. *Phys. Rev. Lett.* **2005,** *95*, 146104.

47. Li, C. P.; Lee, C. S.; Ma, X. L.; Wang, N.; Zhang, R. Q.; Lee, S. T., Growth direction and cross-sectional study of silicon nanowires. *Adv. Mater.* **2003,** *15*, 607-609.

48. Li, F.; Nellist, P. D.; Cockayne, D. J. H., Doping-dependent nanofaceting on silicon nanowire surfaces. *Appl. Phys. Lett.* **2009,** *94*, 263111.

49. Schwarz, K. W.; Tersoff, J.; Kodambaka, S.; Chou, Y. C.; Ross, F. M., Geometrical frustration in nanowire growth. *Phys. Rev. Lett.* **2011,** *107*, 265502.

50. Xu, T.; Nys, J. P.; Addad, A.; Lebedev, O. I.; Urbieta, A.; Salhi, B.; Berthe, M.; Grandidier, B.; Stiévenard, D., Faceted sidewalls of silicon nanowires: Au-induced structural reconstructions and electronic properties. *Phys. Rev. B* **2010,** *81*, 115403.

1
2
3
4
5
6
7
8
9
10
11
12
13
14
15
16
17
18
19
20
21
22
23
24
25
26
27
28
29
30
31
32
33
34
35
36
37
38
39
40
41
42
43
44
45
46
47
48
49
50
51
52
53
54
55
56
57
58
59
60

51. Baski, A. A.; Whitman, L. J., Quasiperiodic nanoscale faceting of high-index Si surfaces. *Phys. Rev. Lett.* **1995,** *74*, 956-959.

52. Baski, A. A.; Whitman, L. J., A scanning tunneling microscopy study of hydrogen adsorption on Si(112). *J. Vac. Sci. Technol. A* **1995,** *13*, 1469-1472.

53. Zhu, Y.; Zhu, Y., Growth property of silicon nanowires under OAG. *Int. J. Mod. Phys. B.* **2005,** *19*, 683-685.

54. Goldthorpe, I. A.; Marshall, A. F.; McIntyre, P. C., Inhibiting strain-induced surface roughening: Dislocation-free Ge/Si and Ge/SiGe core-shell nanowires references. *Nano Lett.* **2009,** *9*, 3715-3719.

55. Allen, J. E.; Perea, D. E.; Hemesath, E. R.; Lauhon, L. J., Nonuniform nanowire doping profiles revealed by quantitative scanning photocurrent microscopy. *Adv. Mater.* **2009,** *21*, 3067-3072.

56. Perea, D. E.; Hemesath, E. R.; Schwalbach, E. J.; Lensch-Falk, J. L.; Voorhees, P. W.; Lauhon, L. J., Direct measurement of dopant distribution in an individual vapour-liquid-solid nanowire. *Nat. Nanotechnol.* **2009,** *4*, 315-319.

57. Buin, A. K.; Verma, A.; Svizhenko, A.; Anantram, M. P., Significant enhancement of hole mobility in [110] silicon nanowires compared to electrons and bulk silicon. *Nano Lett.* **2008,** *8*, 760-765.

58. Murphy-Armando, F.; Fagas, G.; Greer, J. C., Deformation potentials and electron-phonon coupling in silicon nanowires. *Nano Lett.* **2010,** *10*, 869-873.

59. Law, M.; Sirbuly, D. J.; Johnson, J. C.; Goldberger, J.; Saykally, R. J.; Yang, P., Nanoribbon waveguides for subwavelength photonics integration. *Science* **2004,** *305*, 1269-1273.

60. Sun, Y.; Choi, W. M.; Jiang, H.; Huang, Y. Y.; Rogers, J. A., Controlled buckling of semiconductor nanoribbons for stretchable electronics. *Nat. Nanotechnol.* **2006,** *1*, 201-207.

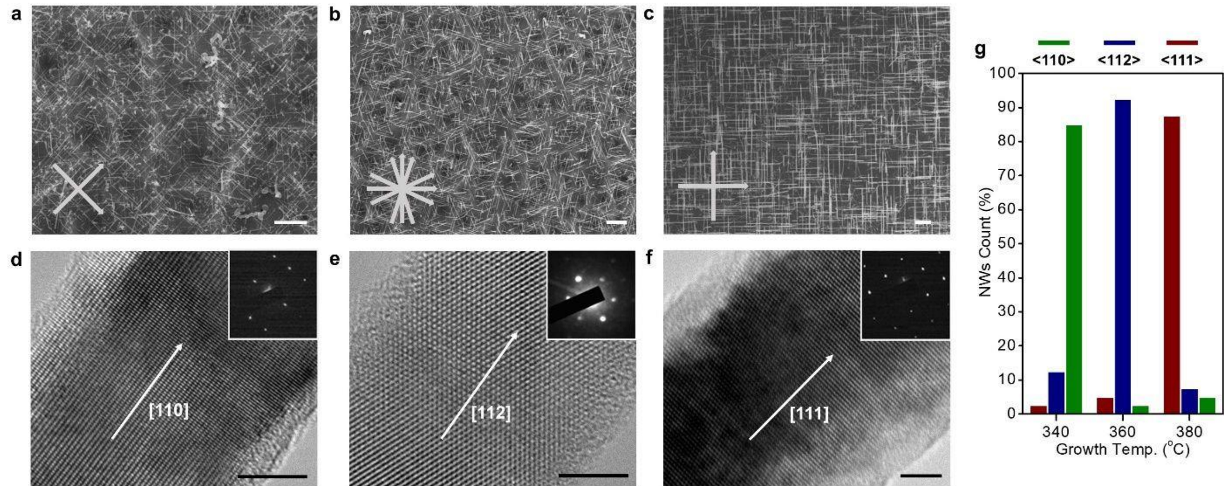

Figure 1. Temperature-dependent growth of <110>, <112>, and <111> oriented GeNWs. Plane-view SEM and HRTEM images with the corresponding SAED patterns of self-catalytic GeNWs epitaxially grown on Ge/Si (100) substrates at different temperatures and growth times with other conditions fixed. (**a** and **d**) <110> oriented GeNWs at 340 °C. (**b** and **e**) <112> oriented GeNWs at 360 °C. (**c** and **f**) <111> oriented GeNWs at 380 °C. Inserts show the schematics of the top view images of the <110>, <112>, and <111> directions on the substrate, respectively. Scale bars (a-c), 1 µm. Scale bar (inset), 500 nm. Scale bars (d-f), 2 nm. (**g**) NW counts versus the corresponding growth temperature to co1ntrol the NW orientation.

1
2
3
4
5
6
7
8
9
10
11
12
13
14
15
16
17
18
19
20
21
22
23
24
25
26
27
28
29
30
31
32
33
34
35
36
37
38
39
40
41
42
43
44
45
46
47
48
49
50
51
52
53
54
55
56
57
58
59
60

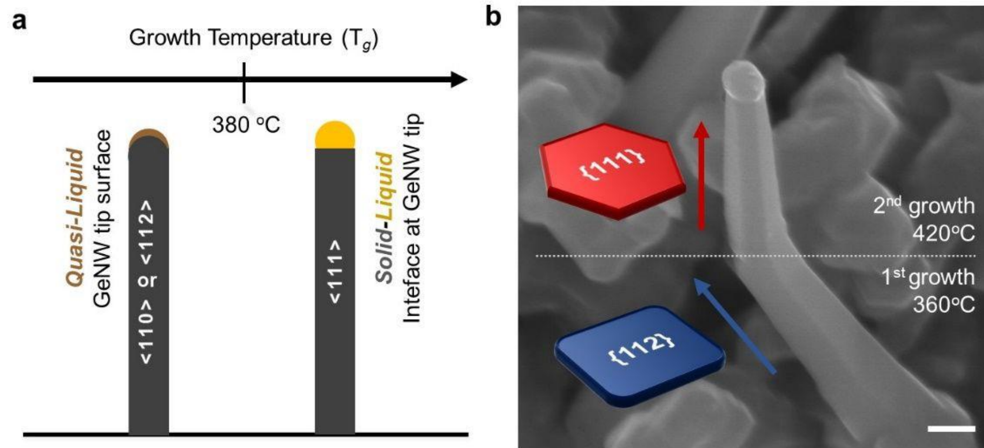

Figure 2. A suggested mechanism for orientation control and growth direction switching of GeNWs. (**a**) Schematic illustration of the self-catalytic growth of GeNWs with a preferential orientation by adjusting growth temperature. (**b**) An SEM image of the kinked GeNW grown by a two-step process, clearly showing the morphological transition from rectangular <112> to hexagonal <111> oriented GeNW. Insets show NW morphologies at the corresponding growth temperatures. Scale bar, 200 nm.

1
2
3
4
5
6
7
8
9
10
11
12
13
14
15
16
17
18
19
20
21
22
23
24
25
26
27
28
29
30
31
32
33
34
35
36
37
38
39
40
41
42
43
44
45
46
47
48
49
50
51
52
53
54
55
56
57
58
60

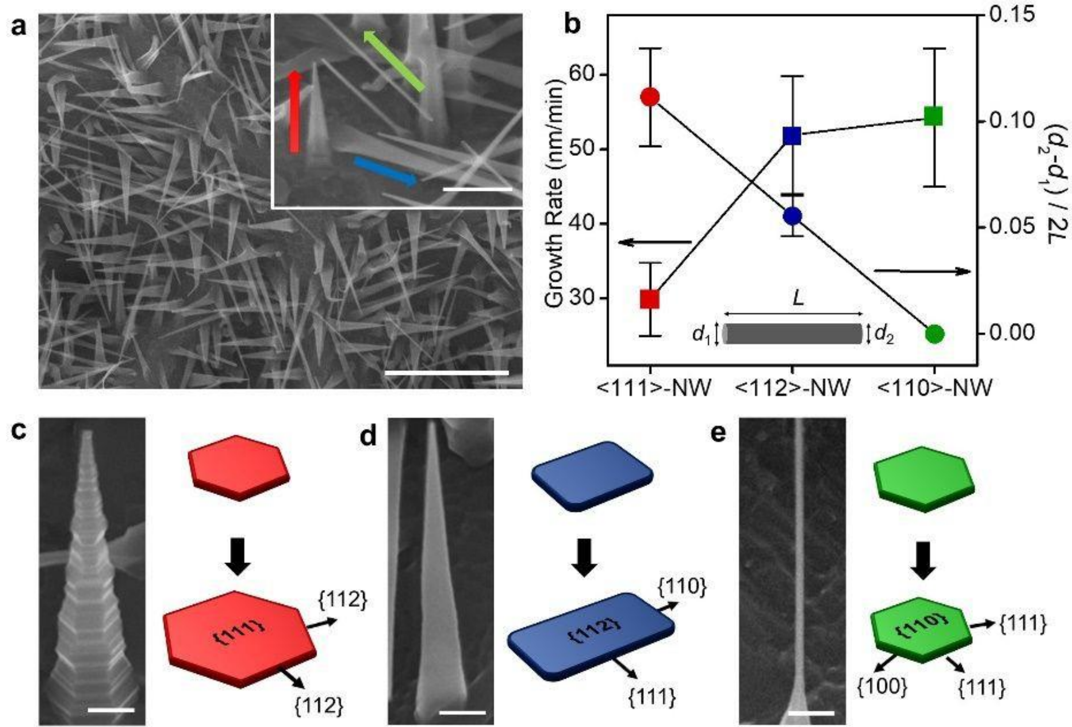

Figure 3. Orientation-dependent structural properties of GeNWs. (**a**) Top-view SEM images of self-catalytic GeNWs grown on Ge/Si(100) substrate at 380 °C with controlled GeH_4 partial pressure of 1.5 Torr. The inset image clearly shows the different NW morphologies and growth rates, dependent on the NW orientations. Scale bars, 200 nm. (**b**) Tapering degree and growth rate variations of GeNWs with different directions at the same growth condition. (**c**, **d**, and **e**) SEM images and schematic models of the <110>, <112>, and <111> oriented NWs exhibiting the different cross-sections and the orientation-modulated change of NW morphologies. Scale bars, 100 nm.

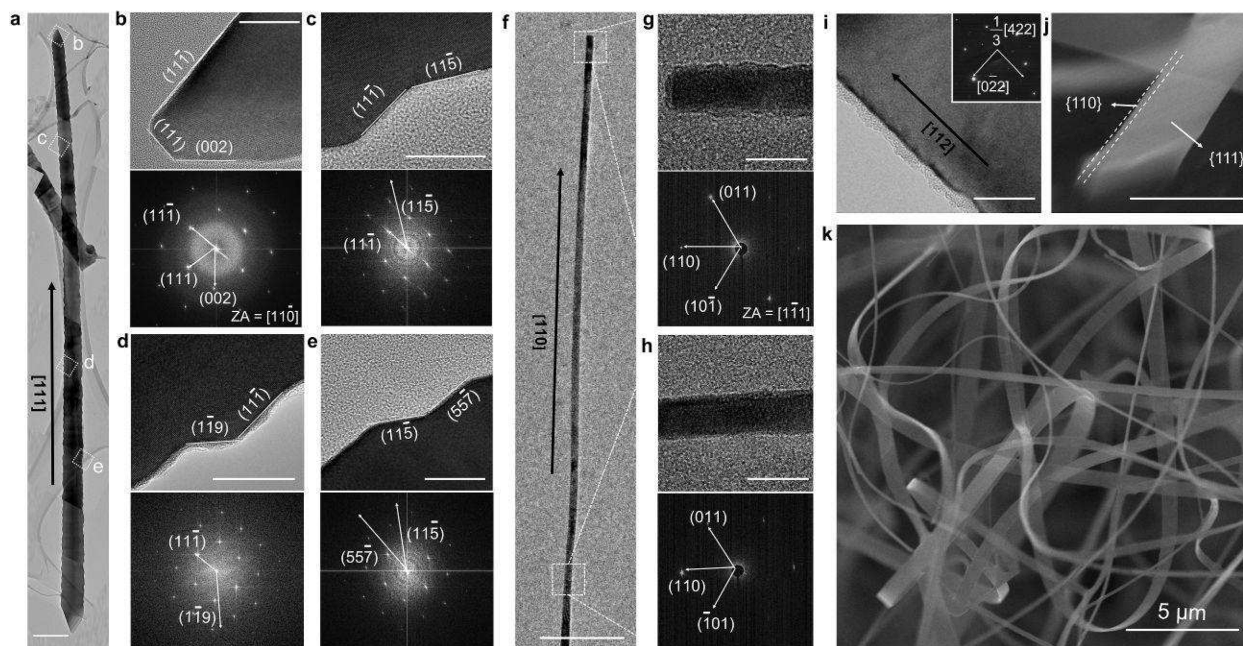

Figure 4. **Crystal structure analysis according to the growth direction of GeNW**. (**a**) Series of TEM and corresponding FFT images showing single crystal [111] oriented NW. Scale bar, 200 nm. (**b**) Tip of GeNW faceted by low-index by low-index (11$\bar{1}$) and (002) planes. (**c**, **d**, and **e**) HR images of the sawtooth faceting with a regular periodicity. (**f**) HR images with the corresponding SAED patterns of [110] oriented GeNW. (**g**) NW growth tip and (**h**) body with an atomically smooth surface. (**i** and **j**) SEM and TEM images of the single crystalline GeNRs, confirming that the GeNRs have a rectangular shape with two {111} and two {110} directions. The inset of (i) is an FFT image corresponding with the same GeNRs. (**k**) SEM image of GeNRs which evolved from <112> oriented GeNWs. Scale bars in (a), (f) and (j), 200 nm. Scale bars in (b-e), (g), (h), and (i), 20 nm.

1
2
3
For Table of Contents Only
4
5
6
7
8
9
10
11
12
13
14
15
16
17
18
19
20
21
22
23
24
25
26
27
28
29
30
31
32
33
34
35
36
37
38
39
40
41
42
43
44
45
46
47
48
49
50
51
52
53
54
55
56
57
58
60